Ultrafast Spectroscopy of the Solvent Dependence of Electron Transfer in a Perylenebisimide Dimer

Michael W. Holman,[†] Ping Yan,[†] David M. Adams,*[,†] Sebastian Westenhoff,[‡] and Carlos Silva[‡,§]

Department of Chemistry, Columbia University, New York, New York 10027, and Cavendish Laboratory, University of Cambridge, Madingley Road, Cambridge CB3 0HE, United Kingdom

Received: January 11, 2005; In Final Form: April 16, 2005

We investigate the photoinduced intramolecular electron-transfer (IET) behavior of a perylenebisimide dimer in a variety of solvents using femtosecond transient absorption spectroscopy. Overlapping photoinduced absorptions and stimulated emission give rise to complicated traces, but they are well fit with a simple kinetic model. IET rates were found to depend heavily on solvent dielectric constant. Good quantitative agreement with rates derived from fluorescence quantum yield and time-resolved fluorescence measurements was found for forward electron transfer and charge recombination rates.

Introduction

Intramolecular electron transfer (IET) is a process of fundamental interest to chemists and physicists,[1−3] which has attracted additional attention due to its relevance to biological systems[4,5] and possible molecular electronic devices.[6,7] Although IET is generally studied in donor−acceptor molecules where the donor and acceptor are different chemical species, symmetry breaking and IET, leading to a charge-separated (CS) state, can also occur in symmetric species under the right conditions.[8−11]

Generally speaking, the possibility of charge separation in such molecules depends on two factors: electronic coupling and solvation. While there must be appreciable electronic overlap of the chromophores for IET to occur within the excited-state lifetime, if the overlap is too great, a lower energy excimer excited state results[12] and charge separation is generally disfavored. Further, even in cases where there is an appropriate amount of coupling, charge separation will still not occur for symmetric molecules in nonpolar solvents; only in higher polarity solvents is the charge-separated state sufficiently stabilized relative to the locally excited state for IET to be energetically favorable.

We have previously studied these effects on electron transfer in symmetric perylenebisimide dimers at the single-molecule level[13,14] and in solution,[15] using steady-state and time-resolved fluorescence spectroscopy. Femtosecond transient absorption (FTA) spectroscopy can provide direct detection of charge-separated states and still more detailed information about the rates and mechanism of rapid forward and back electron transfer.[16−19] We describe here the FTA spectroscopy of the perylenebisimide dimer **D0** in a variety of solvents.

Figure 1 shows the chemical and three-dimensional structure of **D0**, and diagrams the kinetic processes occurring after the photoexcitation. Absorption of a photon leads to a singlet locally excited state, localized at one perylenebisimide (***P**−**P**). The molecule can then relax radiatively to the ground state (k_{fluor}) or undergo electron transfer (k_{et}) to form the charge-separated state ($\mathbf{P}^+-\mathbf{P}^-$). Intersystem crossing, internal conversion, or other nonradiative relaxation processes are slow and generally not observed for these perylenebisimides.[15,20] The charge-separated state can undergo back electron transfer to reform the locally excited state (k_{bet}) or charge recombination to the ground state (k_{cr}).

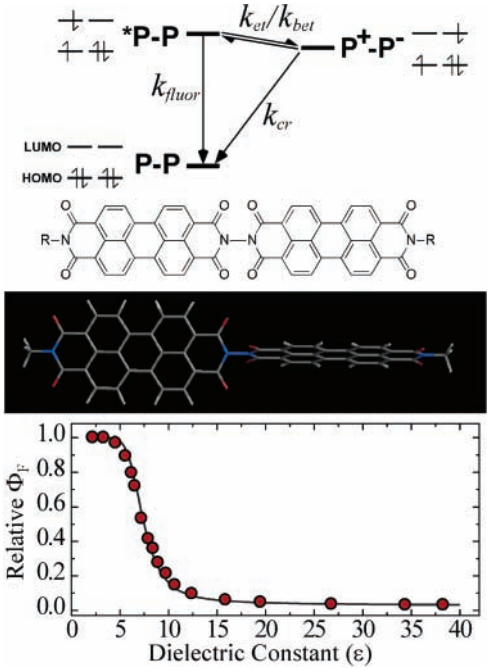

Figure 1. Kinetic scheme for photoinduced intramolecular electron transfer in a perylenebisimide dimer, with the chemical and three-dimensional structures of the dimer **D0**, and the dependence of the relative fluorescence quantum yield on the solvent polarity (dielectric constant); the gray line is a fit using Marcus theory and the kinetic scheme shown above.[15]

The relative energies of the locally excited state (***P**−**P**) and the charge-separated state ($\mathbf{P}^+-\mathbf{P}^-$), and thus $\Delta G_{et}°$ for electron transfer, depend on the solvent polarity. In nonpolar solvents,

* Corresponding author. E-mail: dadams@chem.columbia.edu.
[†] Department of Chemistry, Columbia University, New York, New York 10027.
[‡] Cavendish Laboratory, University of Cambridge, Madingley Road, Cambridge CB3 0HE, United Kingdom.
[§] Current address: Département de physique, Université de Montréal, C.P. 6128, succ. Centreville, Montréal, Québec H3C 3J7, Canada.

10.1021/jp0502050 CCC: $30.25
Published on Web 09/07/2005

charge separation is energetically unfavorable ($\Delta G_{et}^{\circ} > 0$), so k_{et} is slow relative to k_{fluor}, and the equilibrium k_{et}/k_{bet} lies to the left, toward the locally excited state, so essentially no electron transfer is seen. In polar solvents, the charge-separated state is stabilized (so that $\Delta G_{et}^{\circ} < 0$), k_{et} becomes fast relative to k_{fluor}, and the equilibrium k_{et}/k_{bet} lies to the right, meaning that the fluorescence is quenched. Figure 1 shows the dependence of the fluorescence quantum yield on the solvent polarity (dielectric constant),[15] with the dramatic drop in fluorescence due to the increased rate of IET. The shape of the fluorescence spectrum remained the same in all solvents, indicating that all fluorescence is from the locally excited state alone. Fits of these data and fluorescence lifetime measurements can give values for electron-transfer rates, but FTA spectroscopy in polar solvents can detect the perylenebisimide cation and anion and measure IET rates more directly.

Experimental Section

The synthesis of **D0** has been reported previously.[13,21] Steady-state absorption spectra were collected on a PerkinElmer Lambda 25 UV/vis spectrometer, and fluorescence spectra were collected on a PerkinElmer LS 55 luminescence spectrometer. Spectroelectrochemistry was performed using an apparatus described previously.[22]

The femtosecond transient absorption apparatus consisted of a laser system based on the design of Backus et al.[23] Briefly, 15-fs pulses were produced by a mode-locked Ti:sapphire oscillator (KMLabs TS, pumped by 4.5 W, 532 nm output from a Spectra-Physics Millennia V laser). The pulse train was amplified using a chirped-pulse-amplification scheme at a repetition rate of 1 kHz. The amplifier was a multipass Ti:sapphire amplifier (pumped by the 9.5 W, 527 nm output from a Spectra-Physics Evolution X laser). The resulting pulses had a pulse width of 100 fs and a pulse energy of 500 mJ and were centered at a wavelength of 780 nm (1.59 eV photon energy). The sample was excited with pump pulses at 490 nm (2.53 eV photon energy) produced by a collinear optical parameter amplifier (TOPAS). The pump power was varied with calibrated neutral density filters, and the beam was mechanically chopped at 500 Hz. We note that the transient absorption of the samples had a linear dependence on pump power for all of the data shown in this publication. The transient absorption of the sample was probed with a single-filament white-light continuum (approximately from 460 to 950 nm) produced by focusing a fraction of the fundamental into a sapphire window. Probe pulses were delayed with respect to pump pulses with a computer-controlled optical delay. All of the beams were linearly polarized with an angle of 54.7° (magic angle) with respect to each other. The probe beam and a reference beam (not transmitted through the sample) were dispersed in a 0.25-m spectrometer and detected with a pair of avalanche photodiodes (Hamamatsu C5460). The preamplified signal from the diodes was sent to a home-built integrating circuit. Its output voltage is proportional to the area of the diode response and held constant until the next trigger pulse occurs. The integrating circuit output was analyzed using a commercially available Pentium processor with a real-time operating system and 16-bit detection board (processor, NI 8175, 866 MHz PXI embedded controller; detection board, NI PXI-6052E 333kS/s, 16-bit, 16Se/8DI inputs, 24-bit CTR/TMR kit). The computation of $\Delta T/T$ was carried out within the software of the real-time unit. The data were fit using a least-squares method implemented in Microcal Origin 6.0.

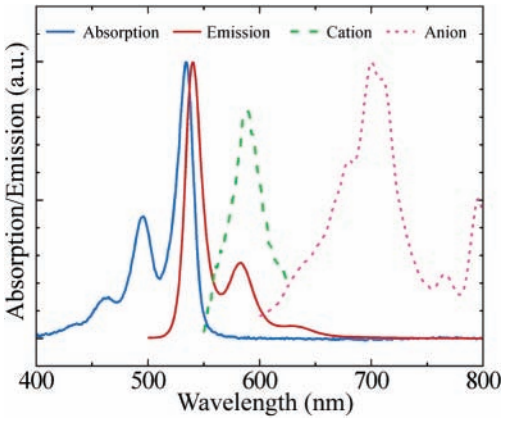

Figure 2. Absorption and emission spectra of **D0**, and the absorption spectra of the electrochemically generated cation and anion of a perylenebisimide monomer; the radical ion spectra are scaled to give an idea of the extinction coefficient relative to the ground-state absorption for a single perylenebisimide chromophore.[20]

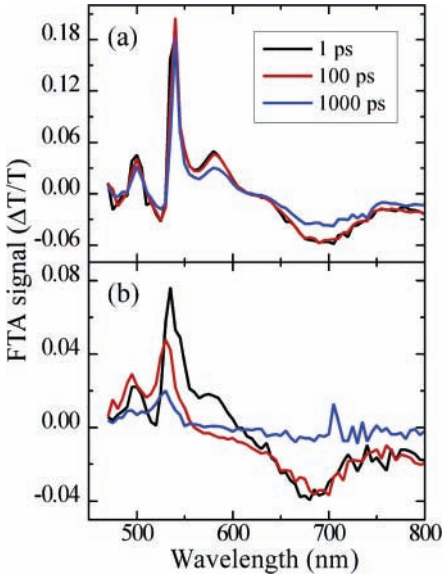

Figure 3. Transient absorption spectra of (a) **D0** in dioxane and (b) **D0** in DMF, at 1 ps (black line), 100 ps (red line), and 1000 ps (blue line) after excitation.

Results and Discussion

Figure 2 shows the steady-state absorption and fluorescence spectra of **D0** in chloroform, with their characteristic vibronic progression and small Stokes shift. These spectra are similar in shape and position to the corresponding spectra of the perylenebisimide monomer in all solvents, indicating that all absorption and emission is to or from the singlet excited state localized at one perylenebisimide chromophore. Figure 2 also shows the absorption spectra of the electrochemically generated cation and anion of a symmetric perylenebisimide monomer (R = 1-hexylheptyl), in excellent agreement with previous reports.[20,24]

Transient absorption spectra of **D0** at 1, 100, and 1000 ps after excitation, in pure 1,4-dioxane (dioxane; low polarity, $\epsilon = 2.21$) and in pure dimethylformamide (DMF; high polarity, $\epsilon = 38.3$), are shown in Figure 3. Both spectra at 1 ps show a positive signal from 470 to 600 nm, resembling a superposition of the steady-state absorption and fluorescence spectra, due the sum of ground-state bleach and the stimulated emission of the locally excited state; and a broad negative signal centered around 680 nm due to excited-state absorption. In dioxane, where **D0** shows no electron transfer ($\Phi_F \approx 1$),[15] the spectrum looks much

TABLE 1: Solvent Dielectric Constants and Parameters Used in Fitting the FTA Data[a]

	dioxane	2:1 acetone:$CHCl_3$	63:37 dioxane:DMF	DMF
ϵ	2.21	1.54	15.6	38.3
k_{fluor}	$4.17 \times 10^8 \pm 1.44 \times 10^8$	4.17×10^8	4.17×10^8	4.17×10^8
k_{et}		$4.87 \times 10^9 \pm 0.24 \times 10^9$	$6.79 \times 10^9 \pm 1.33 \times 10^9$	$8.83 \times 10^9 \pm 3.36 \times 10^9$
k_{bet}		$1.0 \times 10^8 < 4.3 \times 10^8$	$1 \times 10^8 < 2.0 \times 10^9$	$4.83 \times 10^9 \pm 3.57 \times 10^9$
k_{cr}		$4.94 \times 10^8 \pm 1.18 \times 10^8$	$7.87 \times 10^8 \pm 3.62 \times 10^8$	$3.16 \times 10^9 \pm 1.85 \times 10^9$
s_1	0.0471 ± 0.0019	0.0183 ± 0.0005	0.0338 ± 0.0010	0.0102 ± 0.0010
s_2	0.0397 ± 0.0032	0.0136 ± 0.0003	0.0126 ± 0.0010	0.0980 ± 0.0120
s_3		0.0130 ± 0.0004	0.0196 ± 0.0020	0.0000 ± 0.0262
s_4	0.0624 ± 0.0022	0.0331 ± 0.0010	0.0283 ± 0.0022	0.0209 ± 0.0021
s_5		0.0343 ± 0.0019	0.0355 ± 0.0086	0.0306 ± 0.0066

[a] Error limits were estimated by taking upper and lower bounds found to lead to a doubling of the quality of fit parameter χ^2; a "<" sign indicates no lower bound greater than zero was found and that the upper bound is given.

the same at 100 and 1000 ps, decreasing only slightly while having the same shape (the FTA signal does in fact decay at the same rate at all wavelengths, at a rate that agrees with the previously measured radiative rate k_{fluor}, vide infra).

In DMF, however, by 100 ps, the FTA spectrum is very different: the ground-state bleach has increased rather than decreased, the stimulated emission has disappeared and the signal becomes negative above ~560 nm, and the broad absorption around 680 nm has red-shifted slightly. By 1000 ps, almost no signal remains. All of these changes are indicative of the electron transfer, the formation of the charge-separated state ($\mathbf{P}^+-\mathbf{P}^-$) and subsequent charge recombination. In the locally excited state (***P**−**P**), one chromophore is still in the ground state, while in the charge-separated state, neither is, so the charge-separated state should contribute twice as much to the FTA signal of the ground state bleach as the locally excited state. Depletion of the locally excited state, of course, leads to loss of the stimulated emission, and the formation of the cation in the charge-separated state should lead to an absorption around 600 nm (see Figure 2), explaining the negative FTA signal at that wavelength (although the cation absorption spectrum is not fully resolved at 100 ps due to overlap with the residual stimulated emission). Meanwhile, the loss of the locally excited-state absorption around 680 nm is matched by the growth of the anion absorption at 700 nm, leading to the red-shift in the FTA signal.

On the basis of these spectra, we analyze the electron-transfer behavior of **D0** in several solvent systems by taking kinetic traces at or near 500 nm, where the FTA signal is from the ground-state bleach alone, near 600 nm, where the signal is the sum of the stimulated emission and the cation absorption, and near 700 nm, where the signal is the sum of the locally excited state absorption and the anion absorption. Quantitatively,

$$\Delta T/T_{500} = s_1([\mathbf{*P}-\mathbf{P}] + 2[\mathbf{P}^+-\mathbf{P}^-]) \quad (1)$$

$$\Delta T/T_{600} = s_2[\mathbf{*P}-\mathbf{P}] - s_3[\mathbf{P}^+-\mathbf{P}^-] \quad (2)$$

$$\Delta T/T_{700} = -s_4[\mathbf{*P}-\mathbf{P}] - s_5[\mathbf{P}^+-\mathbf{P}^-] \quad (3)$$

where s_1, s_2, s_3, s_4, and s_5 are scaling factors related to the relative extinction coefficients of the various chemical species at the wavelength in question. By our convention, these coefficients are positive and the expected sign of the FTA signal is indicated in eqs 1−3.

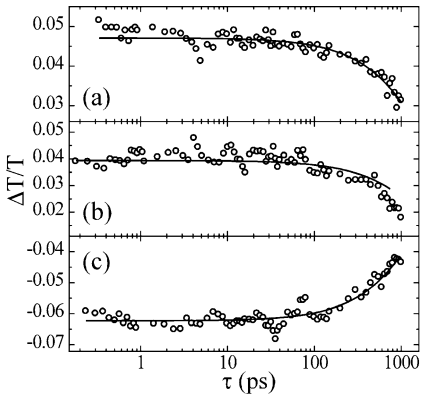

Figure 4. Transient absorption versus time for **D0** in dioxane (ϵ = 2.21) at (a) 500 nm, (b) 580 nm, and (c) 690 nm.

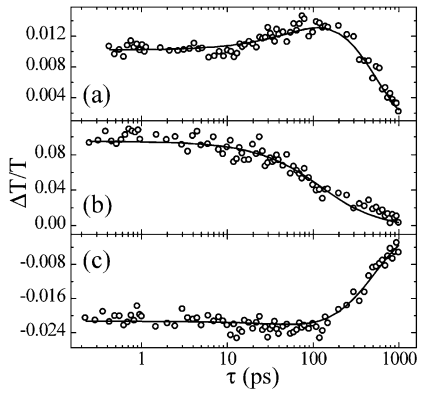

Figure 5. Transient absorption versus time for **D0** in DMF (ϵ = 38.3) at (a) 495 nm, (b) 580 nm, and (c) 685 nm.

The concentrations of the locally excited state and charge-separated state as a function of time can be calculated by adapting known equations for interpreting exciplex kinetics.[25] For the kinetic scheme shown in Figure 1:

$$[\mathbf{*P}-\mathbf{P}] = c_1 e^{-\lambda_1 t} + c_2 e^{-\lambda_2 t} \quad (4)$$

$$[\mathbf{*P}-\mathbf{P}^-] = c_3(e^{-\lambda_1 t} - e^{-\lambda_2 t}) \quad (5)$$

where

$$\lambda_{2,1} = \frac{1}{2}\Big[k_{fluor} + k_{et} + k_{bet} + k_{cr} \pm \sqrt{(k_{vet} + k_{cr} - k_{fluor} - k_{et})^2 + 4k_{et}k_{bet}}\Big] \quad (6)$$

$$c_1 = [\mathbf{*P}-\mathbf{P}]_0(\lambda_2 - k_{fluor} - k_{et})/(\lambda_2 - \lambda_1) \quad (7)$$

$$c_2 = [\mathbf{*P}-\mathbf{P}]_0(k_{fluor} + k_{et} - \lambda_1)/(\lambda_2 - \lambda_1) \quad (8)$$

$$c_3 = [\mathbf{*P}-\mathbf{P}]_0(k_{et})(\lambda_2 - \lambda_1) \quad (9)$$

Equations 1−9 describe the three sets of FTA data as a function of the rates k_{fluor}, k_{et}, k_{bet}, and k_{cr}, and the coefficients s_1−s_5. In practice, the value $[\mathbf{*P}-\mathbf{P}]_0$ is set to one, the coefficients s_1, s_2, and s_4 are set to the initial value of the FTA signal at the relevant wavelength, and k_{fluor} is presumed to be the same in all solvents. Electron-transfer rates are then generated from global fits to all of the FTA data, minimizing the total variance χ^2 for all three

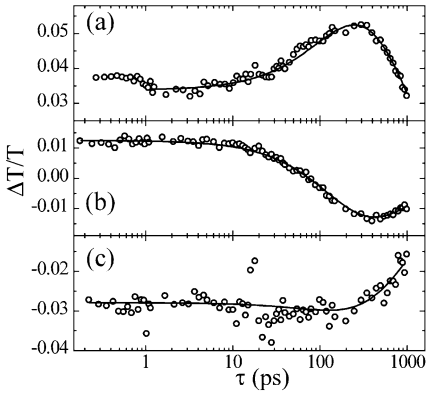

Figure 6. Transient absorption versus time for **D0** in 63:37 dioxane:DMF ($\epsilon = 15.6$) at (a) 505 nm, (b) 600 nm, and (c) 720 nm.

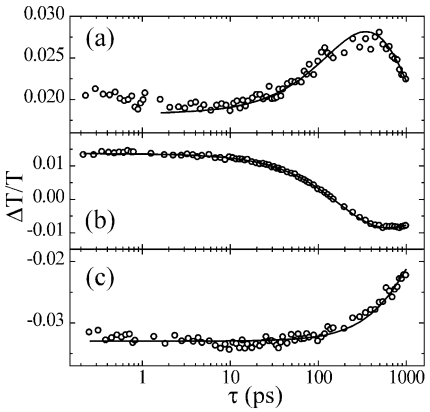

Figure 7. Transient absorption versus time for **D0** in 2:1 acetone:$CHCl_3$ ($\epsilon = 15.4$) at (a) 500 nm, (b) 580 nm, and (c) 700 nm.

curves by varying the rates k_{et}, k_{bet}, and k_{cr}, and the coefficients s_3 and s_5. The results of the fitting are shown in Table 1 and described below.

Figure 4 shows FTA traces for **D0** in dioxane ($\epsilon = 2.21$). Here, no electron transfer occurs, so the data at all three wavelengths decay monoexponentially at essentially the same rate and are best fit by setting all electron-transfer rates to zero, with $k_{fluor} = 4.20 \times 10^8$. This value of k_{fluor} is in general agreement with the value previously reported for **D0** from time-resolved fluorescence experiments[15] and is held constant for **D0** in all other solvents. For **D0** in DMF ($\epsilon = 38.3$), on the other hand, the shapes of the three FTA curves (Figure 5) are quite unusual, because of the overlapping absorptions and emissions described above, but nonetheless they are fit quite accurately by our model.

The electron-transfer behavior was also studied at intermediate polarity, in a mixture of 63:37 dioxane:DMF ($\epsilon \approx 15.6$) (Figure 6) and in a 2:1 acetone:$CHCl_3$ mixture with similar dielectric constant ($\epsilon \approx 15.4$) (Figure 7). The data agree well and are fit with similar values for the rates k_{et}, k_{bet}, and k_{cr}, consistent with our earlier finding that the electron-transfer behavior of perylenebisimide dimers is most often primarily a function of dielectric constant, rather than solvent-specific effects.[15] In these solvents, there is a short, rapid drop in the ground-state bleach FTA signal ($\Delta T/T_{500}$) at <1 ps, which may be due to a small amount of photoionization followed by rapid back electron transfer to the ground state from the solvated electron.[26−29] Because this process is not related to IET, the points below 1 ps for $\Delta T/T_{500}$ were not included when fitting the FTA data.

Figure 8 shows a comparison of the electron-transfer rates calculated here from the FTA data (open shapes) with those found previously[15] from the time-resolved fluorescence data

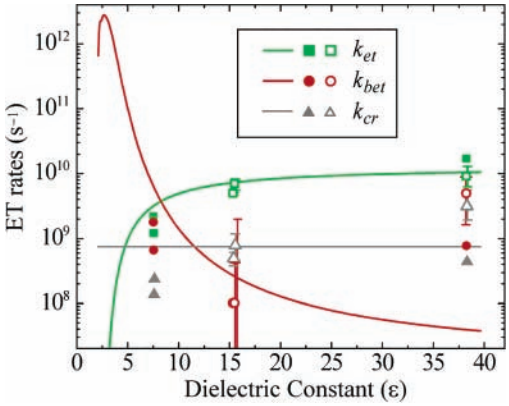

Figure 8. Electron-transfer rates for **D0** as a function of dielectric constant, calculated from FTA data, from the time-resolved fluorescence data (solid shapes) and by fitting the quantum yield versus fluorescence data using Marcus/Jortner theory (lines).[15]

(solid shapes) and by fitting the quantum yield versus fluorescence data using Marcus/Jortner theory (lines). The agreement among all three methods is quite good for k_{et} (green), fairly good for k_{cr} (gray), but not good for k_{bet} (red). This discrepancy is understandable because, for all three methods, the quality of the fits was found to depend most strongly on the value of k_{et}, somewhat less strongly on the value of k_{cr}, and often only very weakly on the value of k_{bet}. For instance, for the FTA data for **D0** in 63:37 dioxane:DMF (Figure 6), changing k_{bet} by a full order of magnitude, from 10^7 to 10^8, changes the total variance χ^2 for all three curves by less than 1%. As such, it is not surprising that values for k_{bet} are unreliable. Given the kinetic model in Figure 1, this weak dependence is understandable, because once the charge-separated state is sufficiently stabilized that $k_{bet} \ll k_{et}$, there is essentially no back electron transfer to the locally excited state and what little there is has only a slight effect on any observable.

Nonetheless, the values for k_{et} and k_{cr} are more reliable and in agreement with our earlier fluorescence measurements on **D0**. The charge recombination rates k_{cr} are consistently slower that the electron-transfer rates k_{et}, even though the former process is far more exothermic, because the charge recombination reaction lies far into the Marcus inverted region[1] (in DMF, $\Delta G_{cr}^{\circ} \approx -2.17$ eV and the total reorganization energy $\lambda \approx 0.95$ eV[15]). These rates also compare well with charge separation and recombination rates measured for a similar symmetric dimer of another perylenebisimide-based chromophore (in 2-methyltetrahydrofuran, $\epsilon = 6.97$),[11] which has somewhat faster rates but also shows charge separation faster than charge recombination.

Conclusion

Photoexcitation can lead to symmetry breaking and charge separation in weakly coupled symmetric dimers if polar solvents sufficiently stabilize the charge-separated state relative to the locally excited state. In this study, photoinduced intramolecular electron transfer in a symmetric perylenebisimide dimer gives rise to transient absorption signals for the perylenebisimide cation and anion. Although absorptions and stimulated emission overlap, fitting the FTA signal versus time at several wavelengths can give rates for the electron-transfer processes occurring after photoexcitation. Rates of forward electron transfer and charge recombination in several solvents of different polarities were found to agree with those found by steady-state and time-resolved fluorescence studies.[15] Rates of back electron transfer to the excited state showed less agreement as extent of

this process is minor under most conditions. The agreement we find among these methods suggests that prospects are strong for both fluorescence and further FTA studies of this and other perylenebisimide-based molecules, or other symmetric species, to better understand the fundamentals of intramolecular electron transfer.

Acknowledgment. Work in Cambridge was supported by the UK Engineering and Physical Sciences Research Council (EPSRC). C.S. received further support from the EPSRC via the Advanced Research Fellowship scheme. Work at Columbia was supported by DOE under award Agency Project # DE-FG02-02ER15375 and partially by NSF MSREC DMR-98-09687. D.M.A. thanks Research Corporation for a Cottrell Scholar award RC#CS0937.

References and Notes

(1) Marcus, R. A. *Annu. Rev. Phys. Chem.* **1964**, *15*, 155−196.
(2) Closs, G. L.; Calcaterra, L. T.; Green, N. J.; Penfield, K. W.; Miller, J. R. *J. Phys. Chem.* **1986**, *90*, 3673−3683.
(3) Adams, D. M.; Brus, L.; Chidsey, C. E. D.; Creager, S.; Creutz, C.; Kagan, C. R.; Kamat, P. V.; Lieberman, M.; Lindsay, S.; Marcus, R. A.; Metzger, R. M.; Michel-Beyerle, M. E.; Miller, J. R.; Newton, M. D.; Rolison, D. R.; Sankey, O.; Schanze, K. S.; Yardley, J.; Zhu, X. *J. Phys. Chem. B* **2003**, *107*, 6668−6907.
(4) McLendon, G. *Acc. Chem. Res.* **1988**, *21*, 160−167.
(5) Gray, H. B.; Winkler, J. R. *Annu. Rev. Biochem.* **1996**, *65*, 537−561.
(6) Joachim, C.; Gimzewski, J. K.; Aviram, A. *Nature* **2000**, *408*, 541−548.
(7) Mantooth, B. A.; Weiss, P. A. *Proc. IEEE* **2003**, *91*, 1785−1802.
(8) Zander, M.; Rettig, W. *Chem. Phys. Lett.* **1984**, *110*, 602−610.
(9) Kang, T. J.; Kahlow, M. A.; Giser, D.; Swallen, S.; Nagarajan, V.; Jarzeba, W.; Barbara, P. F. *J. Phys. Chem.* **1988**, *92*, 6800−6807.
(10) Piet, J. J.; Shuddeboom, W.; Wegewijs, B. R.; Grozema, F. C.; Warman, J. M. *J. Am. Chem. Soc.* **2001**, *123*, 5337−5347.
(11) Giaimo, J. M.; Gusev, A. V.; Wasielewski, M. R. *J. Am. Chem. Soc.* **2002**, *124*, 8530−8531.
(12) Staab, H. A.; Riegler, N.; Diederich, F.; Krieger, C.; Schweitzer, D. *Chem. Ber.* **1984**, *117*, 246−259.
(13) Liu, R.; Holman, M. W.; Zang, L.; Adams, D. M. *J. Phys. Chem. A* **2003**, *107*, 6522−6526.
(14) Holman, M. W.; Adams, D. M. *ChemPhysChem* **2004**, *5*, 1831−1836.
(15) Holman, M. W.; Liu, R.; Zang, L.; Yan, P.; Di Benedetto, S. A.; Bowers, R. D.; Adams, D. M. *J. Am. Chem. Soc.* **2004**, *126*, 16126−16133.
(16) Osuka, A.; Noya, G.; Taniguchi, S.; Okada, T.; Nishimura, Y.; Yamazaki, I.; Mataga, N. *Chem.-Eur. J.* **2000**, *6*, 33−46.
(17) Lukas, A. S.; Zhao, Y.; Miller, S. E.; Wasielewski, M. R. *J. Phys. Chem. B* **2002**, *106*, 1299−1306.
(18) Davis, W. B.; Ratner, M. A.; Wasielewski, M. R. *Chem. Phys.* **2002**, *281*, 333−346.
(19) Guldi, D. M.; Nuber, B.; Bracher, P. J.; Alabi, C. A.; MacMahon, S.; Kukol, J. W.; Wilson, S. R.; Schuster, D. I. *J. Phys. Chem. A* **2003**, *107*, 3215−3221.
(20) Kircher, T.; Lhmannsrben, H.-G. *Phys. Chem. Chem. Phys.* **1999**, *1*, 3987−3992.
(21) Langhals, H.; Jona, W. *Angew. Chem., Int. Ed.* **1998**, *37*, 952−955.
(22) Yan, P.; Holman, M. W.; Robustelli, P.; Chowdhury, A.; Ishak, F. I.; Adams, D. M. *J. Phys. Chem. B* **2005**, *108*, 130−137.
(23) Backus, S.; Durfee, C. G.; Murnane, M. M.; Kapteyn, H. C. *Rev. Sci. Instrum.* **1998**, *69*, 1207−1223.
(24) Gregg, B. A.; Cormier, R. A. *J. Phys. Chem. B* **1998**, *102*, 9952−9957.
(25) Ware, W. R.; Watt, D.; Holmes, J. D. *J. Am. Chem. Soc.* **1974**, *96*, 7853−7860.
(26) Martini, I. B.; Barthel, E. R.; Schwartz, B. J. *J. Chem. Phys.* **2000**, *113*, 11245−57.
(27) Martini, I. B.; Barthel, E. R.; Schwartz, B. J. *Science* **2001**, *293*, 462−465.
(28) Matheson, M. S. Reactions of Solvated Electrons. In *Physical Chemistry: An Advanced Treatise*; Eyring, H., Ed.; Academic Press: New York, 1975; Vol. VII, pp 533−628.
(29) Kee, T. W.; Son, D. H.; Kambhampati, P.; Barbara, P. F. *J. Phys. Chem. A* **2001**, *105*, 8434−8439.